Electron-induced extended-fine-structure measurements of thin-film growth and reaction

Y. U. Idzerda,* Ellen D. Williams, T. L. Einstein, and R. L. Park
Department of Physics and Astronomy, University of Maryland, College Park, Maryland 20742
(Received 5 March 1987)

The application of two electron-beam-induced extended-fine-structure (EFS) techniques [surface extended energy-loss fine structure (SEELFS) and extended appearance-potential fine structure (EAPFS)] to the study of thin films has been demonstrated by measurements on three well-characterized compositional phases of titanium deposited on Si(111). The EFS above the Ti $L_{2,3}$ edge have been measured for an unannealed (20 °C) pure Ti overlayer, a 250 °C-annealed layer (a Si-rich Ti overlayer), and a 400 °C overlayer (a silicide phase). Data were analyzed by using two routines from extended x-ray-absorption fine structure (EXAFS): the standard optical transform (including $\Delta l = +1$ phase shifts) and the ratio method which is independent of phase shifts. The Ti $L_{2,3}$edge EFS satisfies the dipole pseudo-selection-rule of EAPFS, validating the use of $\Delta l = +1$ phase shifts in the EAPFS analysis. The agreement between the measured spectra obtained with SEELFS and EAPFS is very good and is additional confirmation of the use of dipole phase shifts in SEELFS analysis. The nearest-neighbor atomic spacings for both the 20 °C and 250 °C unreacted overlayers were determined by the standard analysis to be 2.93±0.02 Å, in good agreement with the predicted value of 2.915 Å for the two unresolved near-neighbor spacings at 2.89 and 2.94 Å of bulk Ti. Application of the ratio method to this data confirms these results and also shows that the 250 °C-annealed film, measured at room temperature, exhibits a higher degree of structural disorder than the 20 °C film. The absence of additional peaks in the radial distribution function obtained from the EFS and the good straight line fits of the ratio method suggest that the silicon diffuses via grain boundaries. Measurements of the 400 °C data showed a local structure similar to TiSi. The nearest-neighbor pair in this film was determined to be a Ti—Si bond with a spacing of 2.39±0.04 Å, also in good agreement with the predicted value of 2.37 Å, again for two unresolved near-neighbor atomic separations at 2.30 and 2.44 Å of bulk TiSi.

I. INTRODUCTION

Surface extended energy-loss fine structure[1–5] (SEELFS) and extended appearance-potential fine structure[6,7] (EAPFS) are electron-based extended-fine-structure (EFS) techniques which offer many of the analytic capabilities of extended-x-ray-absorption fine structure[8–10] (EXAFS) in an in-house laboratory setting. Both are local-structure probes, sensitive to the near-surface region. Both utilize commercially available, continuously variable, monoenergetic electron sources of high intensity (intensities comparable to synchrotron-based EXAFS, Ref. 11) as well as energy-selective electron detectors. Electron beams can easily be modulated for lock-in detection of the EFS and can also be focused to examine small regions and inhomogeneities or defects on a microscopic scale. In most cases, the same apparatus and chamber used for characterizing the surface (system) can be used for the EFS measurement, simplifying experimental procedures. SEELFS has the additional advantage of being insensitive to the diffraction effects sometimes present in EAPFS.[12]

A significant lingering theoretical problem is the validity of the dipole selection rule in choosing phase shifts to use in the analysis of the EFS data obtained from electron-energy-loss techniques. In the case of EAPFS it is necessary to do explicit calculations of the excitation process to predict the population of each distinct angular momentum final state. Such calculations by Mehl and Einstein[13] show that for the excitation of *nodeless* core states, the final state is dominated by the channel where the change in angular momentum is $\Delta l = +1$. This *nonexclusive* dipole selection rule has been termed a dipole pseudo-selection-rule. In the case of the SEELFS, Leapman[14] has calculated the dependence of the generalized oscillator strength (GOS) on the momentum transfer for several elements. De Crescenzi and Chiarello[2] have emphasized the large contributions of the low-momentum-transfer values in these calculations to the total cross sections, implying the validity of the dipole approximation. Still, no explicit calculations of the relative population of various angular momentum final states by the excited electron have been performed for SEELFS.

Experimental evidence for such a dipole selection rule has been suggested by De Crescenzi and co-workers as a result of SEELFS experiments on the $L_{2,3}$ edge of various materials.[2,4,15,16] These edges have been analyzed using EXAFS-type $\Delta l = +1$ phase shifts and have successfully reproduced the known values for the interatomic spacings of their nearest neighbors. On the other hand, SEELFS measurements on the $M_{2,3}$ edge—for

which the initial core wave function has a node—of other materials[2,4] have consistently resulted in contracted distances of 0.2–0.3 Å from the accepted values. This discrepancy has not been attributed to the incorrect choice of final-state angular momentum, but instead to a failure of the $Z+1$ approximation[17,18] used in calculating the phase shifts utilized in the analysis. The $Z+1$ approximation is not completely applicable in the phase-shift calculations for the low-binding-energy $M_{2,3}$ core level because of the strong interaction of the excited level with the valence electrons. An example of the strength of the interaction can be seen in Fano antiresonances,[19,20] Auger line-shape changes,[21] and charge-transfer excitations which shield the core hole.[22] Nogura and Spanjaard[23] added weight to this claim by demonstrating that the direct recombination of the $M_{2,3}$ core hole with the conduction electrons strongly modifies the $Z+1$ approximation. These results indicate that further calculations for the modifications of the $Z+1$ approximation presented by screening effects are needed for more accurate values for the phase shifts used in EFS analysis of $M_{2,3}$ edges. This additional complication is not specific to electron-beam-based EFS, but would be present in all EFS measurements (including[24] EXAFS) of $M_{2,3}$ core levels.

Tyliszczak and Hitchcock[25] have experimentally pursued the validity of dipole phase shifts by examining the SEELFS of the Ni $M_{2,3}$ edge with a glancing-angle scattering geometry. Restricting the measurement to a small-angle scattering geometry reduces the momentum transfer of the excitation, enhancing its dipole character and altering the contribution of different angular momentum states to the measured EFS. Their results showed no difference in atomic spacings compared to normal-incidence data, suggesting no modification of final angular momentum state contribution.

In comparing the treatments of EAPFS and SEELFS, it is clear that a direct experimental comparison of the EFS measured by SEELFS and EAPFS on a system satisfying the dipole pseudo-selection-rule of EAPFS (for a nodeless core state) would determine to what degree the SEELFS data can be analyzed by dipole selection rule analysis.

An alternative technique used extensively in EXAFS analysis, which avoids the complications due to phase shifts, is the ratio method.[8–10] By comparing the EFS of our unknown sample with that of a similar standard material of known structure, we can determine atomic spacings, coordination number, and relative atomic disorder in our unknown system. In this paper we briefly describe this technique and make the first application of it to SEELFS data to determine atomic spacings independently of phase-shift considerations. The excellent agreement between the ratio method and our standard analysis will further demonstrate the reliability of using dipole phase shifts for SEELFS and EAPFS measured $L_{2,3}$-edge EFS. Additionally, the ratio method has applications beyond the corroboration of the standard analysis results: We used it successfully[3] in the analysis of $M_{2,3}$-edge EFS measurements, where there are no reliable phase-shift values. A major question remaining in the application of the ratio method to $M_{2,3}$-edge data is the transferability of phase shifts. Screening effects which contribute to the failure of the $Z+1$ approximation also undoubtedly affect the central atom phase shifts and may tighten the criteria for phase-shift transferability between systems with different chemical environments.

The near-surface sensitivity of electron-induced EFS techniques makes them ideal for examining the local structure of interacting thin-film systems. In relative terms, the lower electron energy and the elastic scattering nature of EAPFS, which is based on the appearance-potential spectroscopy technique, make it a more surface-sensitive technique than SEELFS.[26] On the other hand, variation of the incident electron energy can be used to effectively vary the surface specificity of SEELFS.

One application of these measurements would be to submonolayer coverages of adsorbed atoms and/or molecules on surfaces. Unfortunately, due to the rapid decline of the total electron cross section with increasing atomic number (and binding energy),[14] we have found that the sensitivity of these techniques using commercial electron sources and detectors is just slightly below the level needed to obtain analyzable EFS for most materials[3] (with the notable exception of very-low-Z elements such as carbon and oxygen). Additional improvements permit submonolayer sensitivity: Signal-to-noise ratio can be increased by reducing unwanted background, using higher incident electron fluxes (with increased attention to possible electron-beam damage of the sample), longer integration periods, and glancing-angle incidence all will increase sensitivity. Our experience has been that EAPFS has a larger signal and higher sensitivity than SEELFS, perhaps due to its higher surface character and reduced background. Promising results for single layers of Co on Si have already been obtained.[16]

Multilayer systems with their inherently more intense and easily observed and analyzed EFS represent a particularly valuable potential application of electron-beam-based EFS techniques. One thin-film system of particular interest is a thin film of titanium deposited on silicon. This system, and its related silicides, have many interesting properties.[27] A deeper understanding of these properties can be obtained from a detailed examination of the interface kinetics leading to the formation of the silicide. A number of recent studies have addressed this concern by examining the microscopic properties of the film and interface. Results show that thick films of titanium deposited in UHV conditions on atomically clean, room-temperature silicon remain essentially unreacted beyond the interface region ($\sim$10 Å). Disagreement remains about the degree and type of intermixing at the interface which occurs during deposition. (In an earlier paper,[28] we found no intermixing at room temperature). If these films are subsequently heated to relatively low temperatures (200 °C), long-range intermixing ($>$100 Å) occurs across the interface. Various techniques show that Si is the dominant diffusing species during intermixing.[29–31] The mechanism for this diffusion has not been determined, although diffusion along grain boundaries[32,33] has

been suggested. At temperatures greater than 500 °C, a stable silicide phase forms which has been identified by x-ray diffraction[27,34] as $TiSi_2$. Unfortunately, due to the absence of long-range order in the overlayer films at the intermediate temperature range (300–500 °C), the constituency and structure of the film at these temperatures remains in dispute. Butz *et al.*, using x-ray diffraction,[34] find that this overlayer is polycrystalline with a very fine grain size (10–30 Å) and a composition close to $TiSi_2$. In contrast, Tromp *et al.*, utilizing high-resolution medium-energy ion scattering (MEIS),[32] suggest that the film composition is TiSi, although no true structure determination was possible. The measurement of local structure in systems lacking long-range order is one of the major strengths of EFS techniques in general. Thus determination of the near-neighbor spacings in these poorly ordered silicide films represents an important test of the applicability of electron-based EFS measurements.

II. EXPERIMENT

The experiments were conducted in an ion and Ti-sublimation pumped UHV system with a base pressure less than 2×10^{-10} Torr. The system is equipped with LEED and Auger electron optics with coaxial electron gun, a single-pass cylindrical mirror analyzer (CMA) with coaxial electron gun which was used for Auger electron spectroscopy (AES), a quadrupole mass spectrometer, a quartz-crystal microbalance (QCMB), and an Ar^+-ion sputtering source. The silicon samples were boron-doped, *p*-type wafers (35–50 Ω cm, 0.4 mm thick) with a (111) orientation. The samples were approximately 1 cm × 1 cm in area and were thermally anchored to a resistive sample heater by a molybdenum clamp and a very small amount of indium inserted between the surface of the heater and the backside of the silicon. There was no evidence of indium segregation from the backside to the Si surface.[35] Temperatures were measured by thermocouples attached to the heaters and were calibrated at high temperature by optical pyrometry.

The Ti films were evaporated onto the Si substrate from a thoroughly outgassed, directly heated Ti-Ta alloy wire. Typical deposition rates were $\frac{1}{3}$ of a monolayer per minute, though uniform deposition rates as low as $\frac{1}{6}$ of a layer per minute and as high as 3 layers per minute were routinely achieved. The Ti deposition rate was measured by a quartz-crystal microbalance to be constant over extended periods (equivalent to >30 layers) but did slowly decrease as the source exhausted its Ti supply. After all depositions, AES again showed only traces of contaminants, and no Ta signal was present in the AES spectra. During deposition, the background pressure remained below 5×10^{-10} Torr.

The SEELFS and EAPFS spectra were measured with the sample at room temperature by simple extensions of standard surface-science techniques, electron-energy-loss spectroscopy[36] (EELS) and disappearance potential spectroscopy (DAPS),[37,38] respectively. In SEELFS, the first- (or second-) derivative electron-energy-loss spectrum for 1–2 keV normally incident electrons is measured using the CMA for energies at, and up to several hundred eV beyond, the Ti $L_{2,3}$ edge (450–850 eV of loss energy). The derivative spectrum is obtained by imposing a 6–10 V peak-to-peak modulating voltage on the gun energy and using lock-in detection techniques. For EAPFS (via DAPS), the LEED optics are used to measure the quasielastic scattering yield as the energy of the electrons incident on the sample is swept through the Ti 2*p* excitation thresholds and beyond the EFS region (450–850-eV range of incident electron energies). Only those electrons that have lost less than a few eV of energy from the incident electron energy (quasielastically scattered electrons) are detected. The first derivative of the quasielastic yield is measured by applying a ~10-V peak-to-peak modulation voltage to the sample potential and using lock-in detection techniques. Additional details of the experimental procedures can be found in the references (SEELFS), (Refs. 1, 3, and 39; EAPFS, Refs. 1, 39, and 40).

We have measured the extended fine structure for three different types of Ti/Si films on Si(111) substrates. Each was formed by deposition of approximately ten layers (25 Å) of Ti at room temperature (RT), quickly heating to a specified temperature for ten minutes and then cooling to room temperature for measurement. The Si and Ti Auger intensities following this procedure for temperatures up to 850 °C are shown in Fig. 1. As described previously,[28,41] the initially deposited Ti forms a smooth film with no intermixing beyond (possibly) the first atomic layer of the Si substrate. The increase in Si intensity at $T\sim200$ °C corresponds to interdiffusion of Si into the Ti film, as described by other workers.[29–31] Above 300 °C, silicide formation begins,[41] resulting in the formation of two stable silicide phases in the *T* ranges labeled III and V in the figure. The EFS measurements were made beyond the Ti $L_{2,3}$ edge (460 eV binding energy) for the as-deposited room-temperature

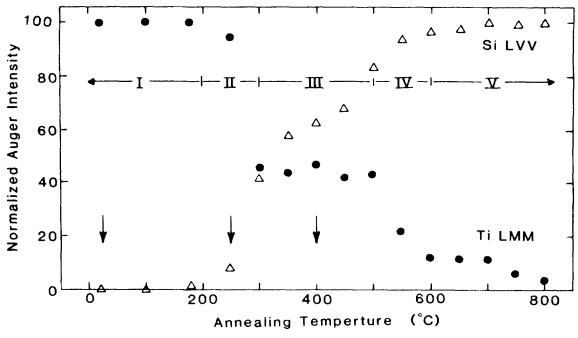

FIG. 1. Normalized Si $L_{2,3}VV$ and Ti $L_3M_{2,3}M_{2,3}$ Auger intensities after 10 min annealing at elevated temperatures for ten layers (25 Å) of Ti on Si(111). Five regions have been indicated as I–V. Regions III (300–500 °C) and V ($\geq$600 °C) display plateaus indicative of the formation of a stable silicide. The arrows at 20 °C, 250 °C, and 400 °C correspond to the annealing temperatures of the samples used for the local-structure determination via SEELFS and EAPFS.

Ti film with a pure Ti composition; the 250 °C Ti overlayer, which exhibits an increased Si content of 15–25 %; and the 400 °C plateau region of the silicide phase. (These annealing temperatures and compositions are indicated by the arrows in Fig. 1.) Difficulties resulting from the reduced EFS signal strength for the $TiSi_2$ overlayer annealed at 650 °C (second plateau region) prevented us from obtaining analyzable EFS for that phase. The drastic reduction in the amplitude of the core loss feature and associated EFS is directly related to the reduction in Ti content within the examined surface region caused by the conversion of the overlayer to $TiSi_2$ and by the coalescence of the silicide into islands.[32] The $TiSi_2$ island formation exposes the bare Si surface and masks a significant fraction of the underlying $TiSi_2$ from our surface probes. The use of thicker silicide films would alleviate this difficulty.

III. RESULTS AND ANALYSIS

The SEELFS and EAPFS of the Ti $L_{2,3}$ edge for the three compositional phases of the Ti/Si system which could be measured are shown in Figs. 2 and 3, respectively. The sharp feature at 560 eV is the L_1 core loss feature. The analysis of the EFS needed to extract the local atomic spacing begins by isolating the EFS features through data truncation and a stiff cubic-spline background subtraction. Then it is integrated (if necessary) to obtain the undifferentiated electron-loss spectrum for

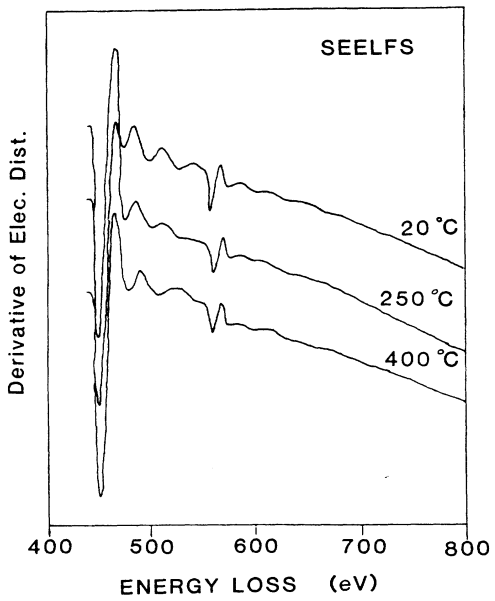

FIG. 2. Three first-derivative, room-temperature SEELFS spectra above the Ti $L_{2,3}$ edge for ten layers of Ti depositied on Si(111) after annealing at the indicated temperatures for 10 min; (a) 20 °C (pure Ti overlayer), (b) 250 °C (Si-rich Ti overlayer), and (c) 400 °C (silicide film). The EFS has been normalized to the measured $L_{2,3}$ core loss intensity. The sharp feature at the loss energy of 560 eV is the L_1 core loss feature.

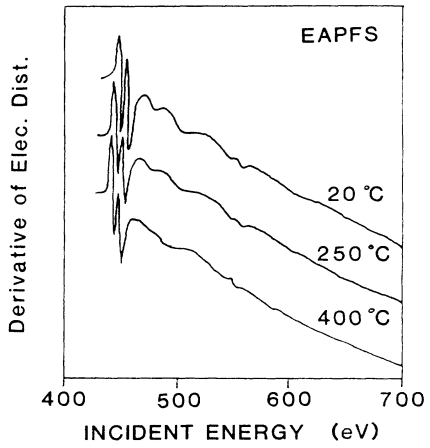

FIG. 3. First-derivative and room-temperature EAPFS measurements after 10-min anneals at the same three temperatures as SEELFS; (a) 20 °C (pure Ti overlayer), (b) 250 °C (Si-rich Ti overlayer), and (c) 400 °C (silicide film). All measurements normalized to the $L_{2,3}$ appearance edge intensity. The sharp feature at 560 eV incident energy is the L_1 appearance edge feature.

SEELFS and the first-derivative electron-energy spectrum for EAPFS. These electron-energy spectra are the proper forms required for strict analogy with EXAFS.[7] First- and second-derivative SEELFS spectra have been utilized to obtain "pseudoradial distribution functions" (PRDF's) (Refs. 1–5) which reproduce known atomic spacings,[2,4] but these PRDF's intensify higher coordination shell contributions as well as complicating k-weighting issues. Data are converted from energy to wave-number dependence using the Lee-Beni method for the determination of the inner potential E_0.[42] A second background subtraction is then performed using a knotted cubic spline. (Variations in the details of the background subtraction result in no significant change in the determination of the atomic spacing.) The wave-number data are weighted by a factor of k^2 to counteract the explicit k^{-1} dependence of the EXAFS equation and the apparent k^{-1} dependence of the Ti or Si backscattering amplitude factor.[17,43]

The weighted data were transformed using an optical Fourier transform to obtain radial distribution functions (RDF's) $F(r)$, which represent the interatomic spacings. The effect of the k weighting and the optical Fourier transform on the EFS is

$$F(r)=\int_{k_{\min}}^{k_{\max}} e^{-i\delta_l(k)}k^2\chi(k)e^{-i2kr}dk\ , \tag{1}$$

where $k_{\min}$ and $k_{\max}$ are the lower and upper limits of the data range and $\chi(k)$ is the background-subtracted EFS in wave-number space. The phase shift correction is included as an exponential term where $\delta_l(k)$ is the energy- and angular-momentum-dependent total phase shift incurred by the excited electron in traversing the atomic potentials of the backscattering and central atoms. We have used the calculated phase shifts of Teo and Lee[17] for the Ti and Si backscattering atom, which

is angular momentum independent, and for the Ti central atom assuming $l=2$ ($\Delta l=+1$). The type of backscattering atom (Ti or Si) is determined by comparing the extracted backscattering amplitude function with theory.[17] We have determined the backscattering atom is Ti for the 20 °C- and 250 °C-annealed data and Si for the 400 °C-annealed data. After these adjustments, peaks in $F(r)$ correspond to the interatomic spacings.

The RDF's for the three examined annealing temperatures are shown in Fig. 4. The similarity between the SEELFS-measured and EAPFS-measured RDF's is apparent. This agreement in the nearest-neighbor atomic spacing for a system where the validity of the use of the dipole phase shifts in EAPFS analysis has been established further corroborates their use in SEELFS analysis. The first peak position for the RT-deposited Ti overlayer *and* the 250 °C-annealed overlayer occurs at 2.93±0.02 Å. This uncertainty reflects the degree of change in the peak position as the background-subtraction parameters are varied. Crystallographic measurements on pure Ti

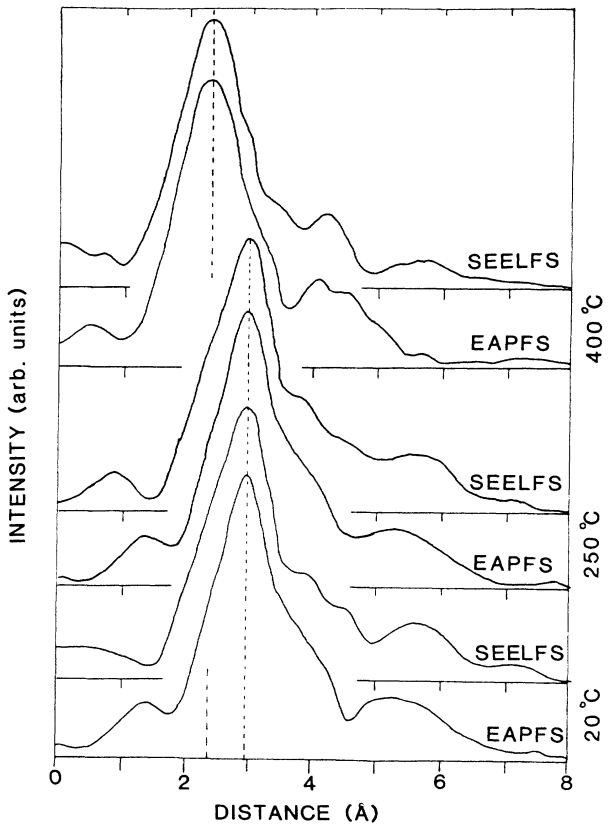

FIG. 4. RDF's for the undifferentiated SEELFS and first-derivative EAPFS-measured EFS for the three annealing temperatures; 20 °C pure Ti overlayer, 250 °C Si-rich Ti overlayer, and 400 °C silicide film. Analysis used $l=2$ phase-shift corrections. The striking overall similarity between the SEELFS and EAPFS RDF's is reflected by the agreement in the first peak positions for all annealing temperatures. First peak positions for both the 20 °C- and 250 °C-annealed films occur at $R=2.93\pm0.04$ Å. The first peak position for the 400 °C-annealed film occurs at $R=2.39\pm0.04$ Å.

indicate that there should be two interatomic spacings very near each other at 2.89 and 2.94 Å,[44] both with a coordination number of 6. These peaks would appear in the RDF as one peak at 2.915 Å. This is very near our value of 2.93 Å and is in good agreement with other EFS measurements for the $L_{2,3}$ edge of pure single-crystal Ti (SEELFS, Ref. 15; EXAFS, Ref. 45) and further confirms our choice of phase shifts.

For the silicide formed at 400 °C, the RDF is quite different from those of the RT or 250 °C data, with a first peak position at 2.39±0.04 Å. For comparison, the local geometry for the three bulk crystal structures of TiSi all contain two nearby Ti-Si atomic spacings at 2.30 and 2.44 Å, again with equal coordination numbers.[44] If these two spacings were not resolved in our EFS measurement (due to the close proximity of these coordination shells, the limited data range, and structural and thermal disordering of the atomic spacings), they would result in an apparent single-shell nearest-neighbor spacing of 2.37 Å. Our single-shell value of 2.39 Å is quite near this expected peak position for TiSi, indicating that the intermediate-temperature film (400 °C) is TiSi. Since there is no evidence for a peak at either the atomic spacing associated with titanium (2.92 Å) or associated with $TiSi_2$ (2.54 Å), the local structure of the titanium atom in the annealed overlayer is TiSi and does not contain a large fraction of other silicide phases. Since the EFS measurements selectively probe the local structure surrounding the Ti atom, these results do not rule out the possibility of additional silicon in the overlayer in excess of the stoichiometric value of TiSi or at the overlayer surface (as indicated by other techniques).

To distinguish among the three TiSi structures, atomic spacing information beyond the nearest-neighbor atoms is required. In our data, there are higher R peaks associated with larger atomic spacings which show qualitative agreement with expected further-neighbor distances for both the Ti and the TiSi. Unfortunately, the positions of these lower-intensity peaks are dependent on our background subtraction, making them unreliable for a quantitative determination of the TiSi crystal structure. Although we are unable to differentiate between the three reported TiSi structures via EFS, the unanalyzed near-edge structure may provide this information as in the case of graphitic carbon on Ni(110).[46]

Additional information about the 250 °C-annealed phase can be obtained through the application of the ratio method to the EFS associated with the first peak for the 20 °C and 250 °C data. In this technique,[8,9] the EFS associated with a single shell from a standard material with known structure is compared with the measured EFS. This comparison can be demonstrated by separating the EFS function into an amplitude term and a phase term. For a single coordination shell,

$$\chi(k)=A(k)\sin(\phi)\ . \tag{2}$$

The amplitude term is given by

$$A(k)=\text{const}\times\frac{N}{R^2}\tau(k)Q(k)\exp(-2R/\lambda)\ , \tag{3}$$

where N is the coordination number of the shell, R is the

coordination shell distance, $r(k)$ is the backscattering amplitude function of the coordination shell atoms, $Q(k)$ is a disorder term (thermal and structural), and λ is the phenomenological mean free path (lifetime) of the electron or core hole state. The phase term is

$$\phi = 2kR + \delta(k) , \tag{4}$$

where k is again the outgoing electron wave number and $\delta(k)$ is the sum of the central atom and backscattering atom phase shifts. Identifying the terms of the EFS equation for the standard with a prime, the total phase difference $\Delta\phi$ between it and the EFS of the measured unknown is

$$\Delta\phi = \phi - \phi' = 2kR - 2k'R' + \delta(k) - \delta'(k') . \tag{5}$$

To the extent that the unknown system and the standard system are similar, the backscattering and central atom phase shifts will be the same and the phase-shift terms will cancel, effectively eliminating the need for any phase-shift corrections in the analysis. We have continued to distinguish between k and k' because of possible difference in the zero of energy, E_0, between the sample and the standard. If this is the case, the intercept of the phase difference $\Delta\phi$ as a function of k will not intersect the origin as it should. By varying $\Delta E_0 = E_0 - E_0'$ until $\Delta\phi$ as a function of k does pass through the origin (modulo 2π), then[9]

$$\delta(k) - \delta(k') = 2(k' - k)R' \tag{6}$$

and

$$\Delta\phi = 2k(R - R') . \tag{7}$$

The slope of this straight line ($\Delta\phi$ versus $2k$) will enable us to extract the difference in interatomic spacing between the unknown and the standard ($R - R'$).

Very significantly, this technique avoids all difficulties associated with the phase shifts. This is especially interesting when applied to the SEELFS technique where questions concerning phase shifts are of paramount importance. Quoted accuracies of this method in EXAFS are often 0.005–0.01 Å (Refs. 8 and 19) for relative interatomic spacing determination. Absolute spacings rely on how well the standard interatomic spacings are known. Any gross deviation from a straight-line fit for $\Delta\phi(k)$ is indicative of nontransferability of the phase shifts[10,47,48] or of too large a non-Gaussian disorder resulting in a significant additional disorder-induced phase shift $\Phi(k)$ (Gaussian disorder creates no additional phase shift[49]). Often a more suitable standard can be found to improve the straight-line fit for these cases.[50]

Further information about the local structure can be obtained by examining the natural logarithm of the ratio of the amplitude functions for the unknown and the standard. For similar sample and standard, both with Gaussian disorder [i.e., $Q(k) = \exp(-\sigma^2 k^2)$], the backscattering amplitude terms cancel giving

$$\ln\left[\frac{A(k)}{A'(k)}\right] = \ln\left[\frac{N/R^2}{N'/(R')^2}\right] - [\sigma^2 - (\sigma')^2]k^2 . \tag{8}$$

Plotting the logarithmic ratio of the amplitudes versus k^2 gives a slope and intercept from which we can determine the unknown coordination number N as well as the disorder information $[\sigma^2 - (\sigma')^2]$.

One complicating factor to the ratio method concerns normalization of the EFS to the core loss feature amplitude. If there is a difference between the number of core excitations in the two EFS measurements, then the plot of the logarithmic ratio of the two EFS amplitudes (which are proportional to the number of excitations) will produce an intercept different than predicted by Eq. (8). (The slope of the logarithmic ratio will, however, be unaffected by this difference.) A method to correct for this error is to normalize the EFS amplitude by the associated core loss intensity (which reflects the number of core excitations). For SEELFS and EAPFS, the data are taken in the derivative mode with inadequate resolution to obtain the true core loss intensity by simple integration. Thus, a separate measurement of the core loss feature under the same electron-beam conditions as the EFS measurements, but with a much improved resolution, is required. To achieve this, we simply reduce the modulation voltage, and therefore the signal intensity, and improve the instrumental resolution. Using a modulation voltage of 1–2 eV for SEELFS and 0.2 eV for EAPFS, the resolution becomes instrument limited at a few eV for the CMA-measured SEELFS (depending on the incident energy) and less than 0.5 eV for EAPFS. Scaling the high-resolution data so that the EFS region intensity matches the larger-modulation-voltage EFS data gives a realistic first-derivative core loss feature which can be integrated to obtain core loss intensity normalization values for the EFS. Even with the improved resolution, there are lingering complications in the normalization procedure such as resonances and associated multielectron excitations which result in core loss features with intensities not proportional to the number of excited electrons.

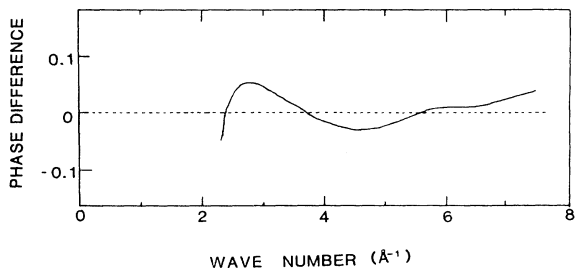

FIG. 5. Total phase difference between the isolated first shell EFS for SEELFS-measured pure Ti overlayer (20 °C) and annealed Si-rich Ti overlayer (250 °C) vs wave number of the excited electron. The dashed line is a least-squares fit to the data (2.5–7.5 $Å^{-1}$). Values for E_0 have been selected that require that the extrapolated straight line intercept the origin at $k=0$. The slope of the straight line, which is twice the difference in atomic spacings, is zero within our uncertainties.

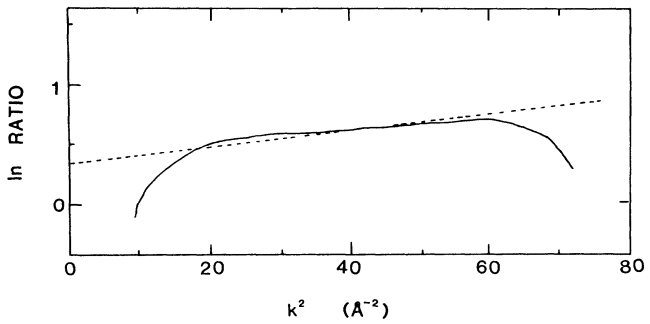

FIG. 6. Log of the ratio of the amplitude of the first shell EFS for the as-deposited pure Ti overlayer (20 °C) and the annealed Si-rich Ti overlayer (259 °C) vs the square of the wave number. The dashed line is a least-squares fit to the data in the range 3–8.5 $Å^{-1}$. The slope is 0.007 ± 0.004 $Å^2$ indicating an increase in disorder for the 250 °C-annealed film.

We have used the ratio method to determine the changes in the Ti film local structure resulting from indiffusion of Si after heating to 250 °C. Thus the as-deposited Ti film was used as the standard. To isolate the EFS associated with a single coordination shell from the remaining shells, the background-subtracted and weighted k-space data was first Fourier transformed directly, without phase shifts. The first peak of the resulting RDF was isolated using a k-space window with sides tapered by a modified Hanning function[51] to minimize truncation effects.[52] The windowed data (consisting of only the first peak) was backtransformed to obtain the EFS associated only with this shell. These EFS spectra were then compared in the ratio method. In Fig. 5 we show the total phase difference versus wave number for the pure Ti overlayer and the Si-rich overlayer. The values for E_0 have been chosen to require that the straight-line fit to the phase difference extrapolate to zero at $k=0$. From the slope of this curve we can determine the atomic spacing difference ΔR. We find essentially no change in atomic spacing of the nearest neighbor for the pure Ti and the Si-rich (250 °C-annealed) Ti overlayers, in agreement with the full analysis using phase shifts.

We have also examined the logarithmic ratio of the EFS amplitude. Figure 6 shows a plot for the ratio of the pure Ti overlayer and the Si-rich Ti overlayer. The slope determined from the straight-line fit gives $\Delta\sigma^2=\sigma^2_{\text{pure Ti}}-\sigma^2_{\text{Si-rich Ti}}=-0.007\pm0.004$ $Å^2$ as the difference in the Debye-Waller-type Gaussian disorders. Since all measurements are made at RT such a value for the Gaussian disorder difference indicates that the Si diffusion into the Ti overlayer creates a structural disruption of the Ti crystalline lattice (similar in magnitude to increases in disorder associated with elevated temperatures of a few hundred degree centigrade[53]). Furthermore, the quality of the fit to a straight line indicates that the backscattering element is the same for the pure Ti overlayer (a Ti backscatterer) and the Si-rich Ti overlayer (where the backscatterer could conceivably be Si instead). Use of the 400 °C-annealed TiSi data, where the backscattering atom is Si, as the standard for comparison with the 250 °C data resulted in very poor fits to a straight line. Thus there is no evidence for the formation of a Ti-Si bond at either the Ti-Si interatomic spacing (present if a silicide is formed) or at the Ti-Ti interatomic spacing (as would occur if a significant fraction of the Ti was replaced by the Si).

Application of the amplitude comparison for a number of similar 250 °C-annealed Ti films all resulted in an increase in σ^2, but the magnitude of the increase ranged from 0.005 to 0.014 $Å^2$. Films annealed at higher temperatures ($T=300$ °C) and exhibiting a larger Si content did not consistently exhibit an increased disorder when compared to a Si-rich Ti overlayer annealed at only 250 °C.

IV. CONCLUSIONS

Our earlier results have shown that thin films (25 Å) of titanium deposited on silicon at room temperature form complete films and remain unreacted. Heat reacting these films to 200–300 °C results in interdiffusion of silicon into the Ti overlayer, but Auger and APS line-shape measurements show that no silicide formation occurs in these moderate-temperature films. Analysis of the electron-beam-induced EFS obtained via SEELFS and EAPFS corroborate these conclusions. The EFS data show that the local environment of the Ti atom after annealing for 10 min at 250 °C remains essentially unchanged compared to that of the pure Ti overlayer. The presence of diffused silicon in the Ti overlayer results in a slight additional disorder in the overlayer, as determined by the increase in σ^2 deduced from the ratio method, but results in no change of atomic spacing. Furthermore, citing the absence of any new peaks in the resulting RDF, and the good straight-line fits of the ratio comparison, the silicon most likely diffuses along grain boundaries rather than substitutionally or interstitially.

Higher-temperature anneals to 400 °C result in the complete formation of a phase which previous studies[34] have shown to lack long-range order. This phase is stable over a range of temperatures but unstable at higher temperatures (> 500 °C) where $TiSi_2$ forms. Distinct changes in DAPS and Auger line-shape spectra are strong indicators of the initiation of the silicide-forming reaction at these elevated temperatures.[41] Analysis of the electron-beam-induced EFS for this phase has shown that the nearest-neighbor pair is a Ti-Si pair with the interatomic spacing consistent with the local structure of TiSi. These results clearly show the power of electron-based EFS techniques to provide otherwise inaccessible information about the processes and structures in thin-film growth. Furthermore, our results are further confirmation of the applicability of dipole phase shifts in the SEELFS analysis. The good agreement between the RDF's for the SEELFS and EAPFS on a core state which satisfies the dipole pseudo-selection-rule criteria of EAPFS strongly suggests at least a similar dipole selection rule for SEELFS phase shifts.

ACKNOWLEDGMENTS

We thank Jouko Vähäkangas and Dan Abell for their assistance in the taking of the measurements. Computer facilities were supplied by the University of Maryland Computer Science Center. This work supported by a grant from Martin Marietta Laboratories and by National Science Foundation Grant No. DMR-85-51436. One of us (T.L.E.) was partially supported by the U.S. Department of Energy (DOE) under Grant No. DE-FG05-84ER45071.

*Present address: Condensed Matter and Radiation Science Division (Code 4635.I), Naval Research Laboratory, Washington, D.C. 20375-5000.

[1]Y. U. Idzerda, Ph.D. dissertation, University of Maryland, 1986 (unpublished).
[2]M. De Crescenzi and G. Chiarello, J. Phys. C **18**, 3595 (1985).
[3]Y. U. Idzerda, E. D. Williams, T. L. Einstein, and R. L. Park, Surf. Sci. **160**, 75 (1985).
[4]M. De Crescenzi, Surf. Sci. **162**, 838 (1985).
[5]A. P. Hitchcock and C. H. Teng, Surf. Sci. **149**, 558 (1985).
[6]M. L. den Boer, T. L. Einstein, W. T. Elam, R. L. Park, L. D. Roelofs, and G. E. Laramore, Phys. Rev. Lett. **44**, 496 (1980).
[7]P. I. Cohen, T. L. Einstein, W. T. Elam, Y. Fukuda, and R. L. Park, Appl. Surf. Sci. **1**, 538 (1978).
[8]P. A. Lee, P. H. Citrin, P. Eisenberger, and B. M. Kincaid, Rev. Mod. Phys. **53**, 769 (1981).
[9]B. K. Teo, *EXAFS: Basic Principles and Data Analysis*, Vol. 9 of *Inorganic Chemistry Concepts* (Springer-Verlag, New York, 1986).
[10]E. A. Stern and S. M. Heald, in *Handbook of Synchrotron Radiation*, edited by E. E. Koch (North-Holland, Amsterdam, 1981), Vol. 1.
[11]R. D. Leapman, L. A. Grunes, P. L. Fejes, and J. Silcox, in *EXAFS Spectroscopy, Techniques and Applications*, edited by B. K. Teo and D. C. Joy (Plenum, New York, 1981), p. 217.
[12]T. L. Einstein, M. L. den Boer, J. F. Morar, R. L. Park, and G. E. Laramore, J. Vac. Sci. Technol. **18**, 490 (1981).
[13]M. J. Mehl, T. L. Einstein, and G. W. Bryant, J. Vac. Sci. Technol. A **2**, 862 (1984); M. J. Mehl and T. L. Einstein (unpublished).
[14]R. D. Leapman, P. Rez, and D. F. Mayers, J. Chem. Phys. **72**, 1232 (1980).
[15]M. De Crescenzi, G. Chiarello, E. Colavita, and R. Memeo, Phys. Rev. B **29**, 3730 (1984).
[16]E. Chainet, M. De Crescenzi, J. Derrien, T. T. A. Nguyen, and R. C. Cinti, Surf. Sci. **168**, 801 (1986).
[17]See, for example, B. K. Teo and P. A. Lee, J. Am. Chem. Soc. **101**, 2815 (1979), and references therein.
[18]B. E. Chainet, M. De Crescenzi, and J. Derrien, Phys. Rev. B **31**, 7469 (1985).
[19]C. U. Fano, Phys. Rev. **124**, 1866 (1961).
[20]D. R. E. Dietz, E. G. McRae, and J. H. Weaver, Phys. Rev. B **21**, 2229 (1980).
[21]E. G. Ertl and J. Küppers, *Low Energy Electrons and Surface Chemistry Analysis* (Chemie, Weinheim, 1974), p. 33.
[22]T. H. Carlson, *Photoelectron and Auger Spectroscopy* (Plenum, New York, 1975).
[23]F. C. Noguera and D. Spanjaard, J. Phys. F **11**, 1183 (1981).
[24]S. Modesti, M. Fanfoni, M. De Crescenzi, N. Motta, and R. Rosei, Phys. Rev. B **32**, 7826 (1985).
[25]T. Tyliszczak and A. P. Hitchcock, J. Vac. Sci. Technol. A **4**, 1372 (1986).
[26]K. Nishimori, H. Tokutaka, and K. Takashima, Surf. Sci. **100**, 665 (1980).
[27]S. P. Murarka and D. B. Fraser, J. Appl. Phys. **51**, 342 (1980).
[28]J. Vahakangas, Y. U. Idzerda, E. D. Williams, and R. L. Park, Phys. Rev. B **33**, 8716 (1986).
[29]W. K. Chu, S. S. Lau, J. W. Mayer, H. Muller, and K. N. Tu, Thin Solid Films **25**, 393 (1975).
[30]A. P. Botha and R. Pretorius, Thin Solid Films **93**, 127 (1982).
[31]P. Revesz, J. Gyimesi, L. Pogany, and G. Pëto, J. Appl. Phys. **54**, 2114 (1983).
[32]R. M. Tromp, G. W. Rubloff, and E. J. van Loenen, J. Vac. Sci. Technol. A **4**, 865 (1986); G. W. Rubloff, R. M. Tromp, and E. J. van Loenen, Appl. Phys. Lett. **48**, 1600 (1986).
[33]R. Butz, G. W. Rubloff, and P. S. Ho, J. Vac. Sci. Technol. A **1**, 771 (1983).
[34]R. Butz, G. W. Rubloff, T. Y. Tan, and P. S. Ho, Phys. Rev. B **30**, 5421 (1984).
[35]J. J. Lander and J. Morrison, Surf. Sci. **2**, 553 (1964).
[36]E. G. Ertl and J. Küppers, *Low Energy Electrons and Surface Chemistry Analysis* (Chemie, Weinheim, 1974), p. 53.
[37]L. Kirshner and P. Staib, Appl. Phys. **6**, 99 (1975).
[38]M. L. den Boer, P. I. Cohen, and R. L. Park, Surf. Sci. **70**, 643 (1978).
[39]Y. U. Idzerda, E. D. Williams, T. L. Einstein, and R. L. Park, J. Vac. Sci. Technol. A **5**, 847 (1987).
[40]Robert L. Park and J. E. Houston, J. Vac. Sci. Technol. **11**, 1 (1974), and references therein.
[41]Y. U. Idzerda, E. D. Willams, R. L. Park, and J. Vähäkangas, Surf. Sci. Lett. **177**, L1028 (1986).
[42]P. A. Lee and G. Beni, Phys. Rev. B **15**, 2862 (1977).
[43]P. A. Lee and J. B. Pendry, Phys. Rev. B **11**, 2795 (1975).
[44]W. B. Pearson, *A Handbook of Lattice Spacings and Structures of Metals and Alloys* (Pergamon, London, 1967), Vol. 2.
[45]D. Denley, R. S. Williams, P. Perfetti, D. A. Shirley, and J. Stöhr, Phys. Rev. B **19**, 1762 (1979).
[46]L. Papagno and L. Caputi, Phys. Rev. B **29**, 1483 (1984).
[47]P. H. Citrin, P. Eisenberger, and B. M. Kincaid, Phys. Rev. Lett. **36**, 1346 (1976).
[48]B. A. Bunker and E. A. Stern, Phys. Rev. B **27**, 1017 (1983).
[49]P. Eisenberger and G. S. Brown, Solid State Commun. **29**, 481 (1979).
[50]E. A. Stern, B. A. Bunker, and S. M. Heald, Phys. Rev. B **21**, 5521 (1980).
[51]W. T. Elam, Ph.D. thesis, University of Maryland, 1979 (unpublished).
[52]J. Stöhr, R. Jaeger, and S. Brennan, Surf. Sci. **117**, 503 (1982).
[53]E. A. Stern, D. E. Sayers, and F. W. Lytle, Phys. Rev. B **11**, 4836 (1975).